

## Embryology of *Helianthus annuus* (Asteraceae)

Marina M. Gotelli<sup>1,2,\*</sup>, Beatriz G. Galati<sup>1</sup> & Diego Medan<sup>2</sup>

<sup>1)</sup> Laboratorio de Biología Reproductiva en Plantas Vasculares (79), Facultad de Ciencias Exactas y Naturales, Universidad de Buenos Aires, Argentina (\*corresponding author's e-mail: mgotelli@bg.fcen.uba.ar)

<sup>2)</sup> Grupo de Biología Reproductiva en Plantas Superiores, Cátedra de Botánica Agrícola, Facultad de Agronomía, Universidad de Buenos Aires, Argentina

Received 13 Nov. 2006, revised version received 10 Apr. 2007, accepted 17 Apr. 2007

Gotelli, M. M., Galati, B. G. & Medan, D. 2008: Embryology of *Helianthus annuus* (Asteraceae). — Ann. Bot. Fennici 45: 81–96.

Abortion of sunflower fruits during different phases of their development could be due to abnormalities in the reproductive process. We report a comparative study of the sporogenesis, gametogenesis and the development of the related sporophytic structures in three commercial hybrids, DK 4050, CF 17 and P30, and a line, HA 89. The anther wall consists of epidermis, endothecium, one middle layer and a plasmodial tapetum with binucleate cells before integrating. A peritapetal membrane with orbicules encloses the pollen grains, which are triporate, angulaperturate and shed at tricellular stage. HA 89 also presents tetraporate pollen grains. The ovule is tenuinucellate, unitegmis and anatropous. The young female gametophyte consists of six cells and eight nuclei. Antipodals, which vary in number and in the number of nuclei in each cell, usually have thick walls between themselves and the central cell. Differences among the genotypes studied may explain the contradictions found on previous accounts.

Key words: embryology, gametogenesis, *Helianthus annuus*, sporogenesis

### Introduction

There are several embryological studies on the sunflower, *Helianthus annuus* (Asteraceae). The development of the female gametophyte before and after fertilization was investigated with the light and electron microscope (Ustinova as cited in Newcomb 1972a, 1972b, Yan *et al.* 1990). Comparative accounts of microsporogenesis in male-fertile and cytoplasmic male-sterile flowers were reported by Horner (1977), Szabó *et al.* (1984) and Laveau *et al.* (1989). However, only in very few investigations were the genotypes specified. Moreover, the information available

on the subject presents many contradictions, and development in commercial hybrids is for the most part unknown.

The abortion of sunflower fruits during different phases of their development could be due to abnormalities in the reproductive process, regardless of the physiological aspects. The embryology of three commercial hybrids and a line of *Helianthus annuus* were comparatively studied as part of a research for the possible causes of fruit abortion and in order to contribute to the anatomical characterization of the flowers that produce viable seeds.

## Material and methods

Three commercial hybrids of sunflower, P 30, DK 4050 and CF 17 and a line, HA 89, were grown under natural conditions in the province of Buenos Aires, Argentina, during the summer of 2001–2002. Approximately one hundred flowers of each genotype in different stages of development (between floral primordial and anthesis) were fixed in FAA and embedded in paraffin. Sections (5–10  $\mu\text{m}$ ) were cut and stained with safranin combined with fast green (D'Ambrogio 1986) and observed with a Wild M20 microscope. Photographs were taken with a manual camera adapted to a Zeiss microscope. For SEM studies pollen grains were dehydrated in an ascendant series of acetone (70%, 80%, 90%, 100%), sputtercoated with gold-palladium for 3 min (O'Brien and McCully 1981) and observed with a SEM Philips Series XL, Model 30.

## Results

### Microsporangium

The young anther wall consists of epidermis, endothecium, one middle layer and tapetum (Figs. 1C, 2C, 3C). The anther wall development is of the dicotyledonous type (Davis 1966) since the middle layer and the endothecium share the same origin (Figs. 1A, 2A, 3A).

In floral primordia, cells that form the four wall layers are of similar size and shape. Tapetum cells are the first to enlarge and become binucleate at microspore mother cell stage. These cells have a dense cytoplasm with calcium oxalate styloid crystals (Figs. 1A–C, 2A–C, 3A–C). During microsporogenesis the inner tangential and radial walls of the tapetal cells break down. With the release of microspores from the tetrads the outer tangential wall also disappears to form a periplasmodium that surrounds the young unicellular microspores (Figs. 1C, D, 2C, D, 3C, D, 4D). The plasmodium is completely integrated at bicellular pollen-grain stage. The styloid crystals at this stage are larger in DK 4050 (23  $\mu\text{m}$ ) than in HA 89 (8  $\mu\text{m}$ ), while in CF 17 and P 30 they are absent. The tapetum is gradually consumed and no longer present when pollen grains reach

the mature bicellular stage (Figs. 1E, F, 2E, 3E, 4E, F).

Simultaneously, a peritapetal membrane is formed towards the middle layer. This membrane encloses the mature pollen grains (Fig. 5C). Ubisch bodies of approximately 0.32  $\mu\text{m}$  are attached to the inner surface of it (Fig. 5A and B).

After the first meiotic division, the middle layer cells start a slow degeneration process. At late tetrad stage most of these cells have been disintegrated and are no longer found at the young microspore stage (Figs. 1C, 2C, 3C). Fibrous thickenings develop from the inner tangential and radial walls of the endothecium cells during microgametogenesis. These thickenings are interrupted in the outer tangential face (Figs. 1E, F, 2D, E, 3E, 4E). Therefore, the endothecium acts mechanically in the dehiscence of the anther. In CF 17 and P 30 such thickenings are already developed at the young bicellular pollen grain stage, while the tapetum is still present (Fig. 2D). Prismatic and styloid crystals were only observed in young endothelial cells of HA 89 (Fig. 1C–F) and mature cells of DK 4050 (Fig. 3E). Epidermal cells grow tangentially as the anther matures. A thick cuticle occurs at the same stages in which the endothelial thickenings are present (Figs. 1E, F, 2D, E, 3E).

### Microsporogenesis and microgametogenesis

The sporogenous tissue differentiates once the four layers of the anther wall are formed. This tissue is distinguishable by the presence of few intercellular spaces and by isodiametric cells with prominent nuclei and thin walls. Microspore mother cell walls become thicker due to deposition of callose between the plasmalemma and the primary wall (Figs. 1A, 2A, 3A, 4A). Subsequently, they come apart by dissolution of the middle lamella and primary walls that keep the sporogenous tissue together. Each microspore mother cell undergoes simultaneous reductive divisions and gives rise to microspore tetrads with tetrahedral arrangement (Figs. 1B, 2B, 3B, 4B).

Each individual microspore becomes sepa-

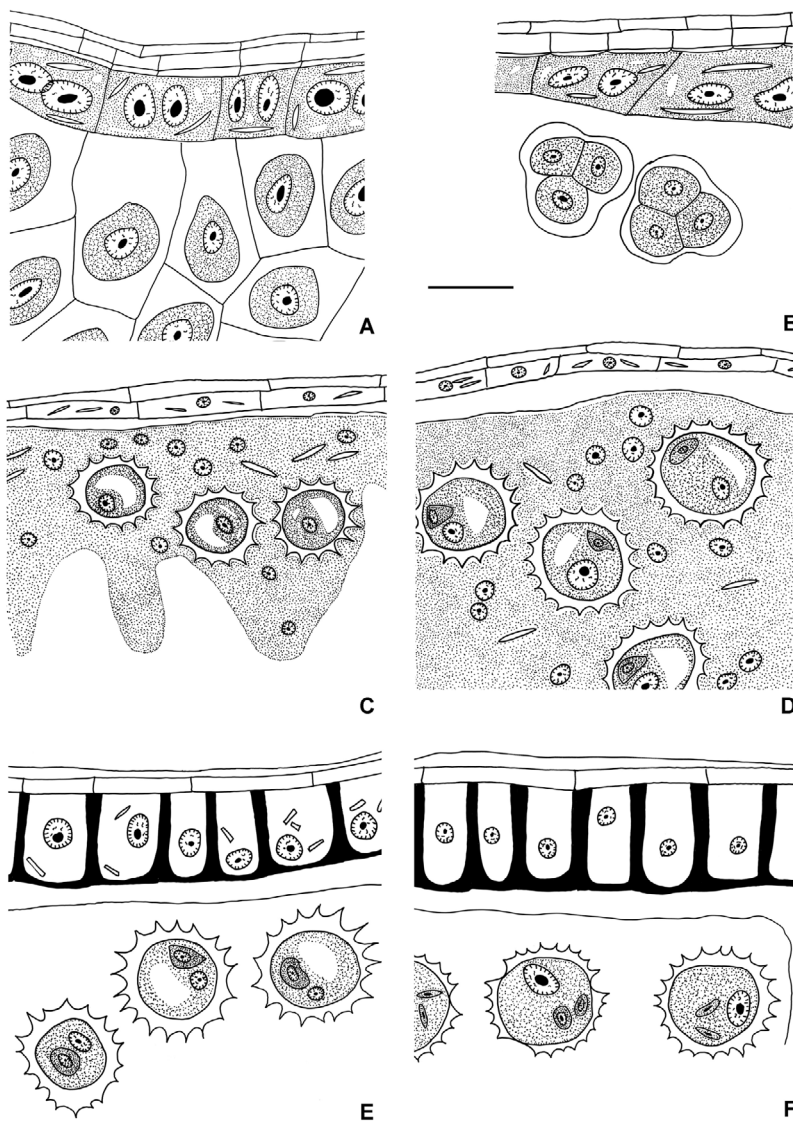


**Fig. 1.** *Helianthus annuus* (HA 89). Microsporangium tissues in different stages of development. — **A:** Microspore mother cell stage, binucleate tapetum with styloid crystals. — **B:** Tetrahedral tetrads, middle layer mostly degraded. — **C:** Free microspore stage, styloid crystals in endothecium cells and in the developing plasmodial tapetum. — **D:** Young bicellular pollen-grain stage, plasmodial tapetum totally integrated. — **E:** Late bicellular pollen-grain stage, thick epidermal cuticle visible, endothecium cells with fibrous thickenings and prismatic crystals, tapetum completely consumed, peritapetal membrane present. — **F:** Three-celled pollen grains, endothecial cells without crystals. Scale bar 18  $\mu\text{m}$ .

rated from the tetrad by a sudden dissolution of the callose wall. Deposition of sporopollenin begins immediately after the release of microspores into the anther locule. Consequently a thick exine wall is formed. Young uninucleate microspores show a vacuolated cytoplasm. CF 17 and P 30 present smaller free microspores than HA 89 and DK 4050 (Figs. 1C, 2C, 3C, 4C).

The first division of the microspore gives rise to a small generative cell and a large vegetative cell. The former separates from the intine and moves to a position where it is enclosed by the

latter. Soon after pollen grains are formed they increase their volume, which generates a stretching and slimming of the exine. Young bicellular pollen grains of DK 4050 are smaller (19  $\mu\text{m}$ ) and less vacuolated than in the other genotypes (30  $\mu\text{m}$ ) (Figs. 1D, 2D, 3D). The vegetative cell continues to grow, the vacuole gradually disappears, and the cytoplasm becomes filled with starch grains. Finally, two sperm cells are formed by the mitotic division of the generative cell. The hybrids have larger mature three-celled pollen grains than the line (Figs. 1F, 2E, 3E). At this stage, the pollen grains are shed.

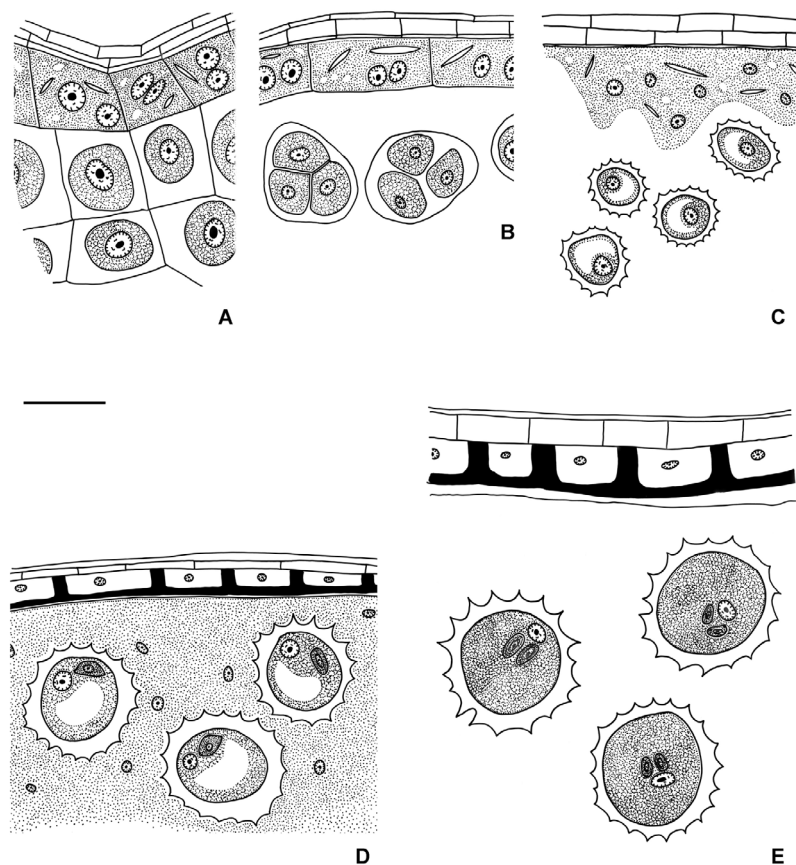


**Fig. 2.** *Helianthus annuus* (CF 17 and P 30). Microsporangium tissues in different stages of development. — **A:** Microspore mother cell stage, binucleate tapetum with styloid crystals. — **B:** Tetrahedral tetrads, middle layer mostly degraded. — **C:** Free microspore stage, tapetum invading the anther locule. — **D:** Bicellular pollen-grain stage, thick epidermal cuticle visible, endothecium cells with fibrous thickenings, tapetum completely integrated without crystals. — **E:** Three-celled pollen grains, peritapetal membrane present. Scale bar 18  $\mu\text{m}$ .

## Pollen grain morphology

Mature pollen grains are suboblate, triporate and angulaperturate with spherical amb. In HA 89 tetraporate pollen grains were also found (Fig. 4F). Mesocolpia, as well as apocolpia of all genotypes, present an echinate tectum surface (Fig. 5C) with spread microperforations on the base of each spine (Fig. 5D).

## Gynoecium

The gynoecium is usually bicarpelar and unilocular with one ovule per ovary. The style is apically inserted and the stigma is bifid. However, flowers with more than one ovule per locule and more than one locule were found in approximately 5% of the flowers. These may have one or two styles, not necessarily in concordance with the number of ovules or locules. The stigma

surface is papillose. The style is solid with a central strand of elongated cells that constitutes the transmitting tissue.

## Ovule

The mature ovule is anatropous, unitegmic and tenuinucellate (Figs. 6A, 8A, 10A). Cells of the inner epidermis of the integument during early stages of ovule development elongate radially, acquire a dense cytoplasm, show prominent nuclei and differentiate into an endothelium. In DK 4050, at megaspore mother cell stage, this tissue comprises a single layer of uninucleate cells (Fig. 10B). In CF 17, P 30 and HA 89 the endothelium was not observed at such stage of ovule development. In all the genotypes the studied cells of the endothelium had up to three nuclei at the megaspore tetrad stage and during the gametophyte development (Figs. 6B, 8B,



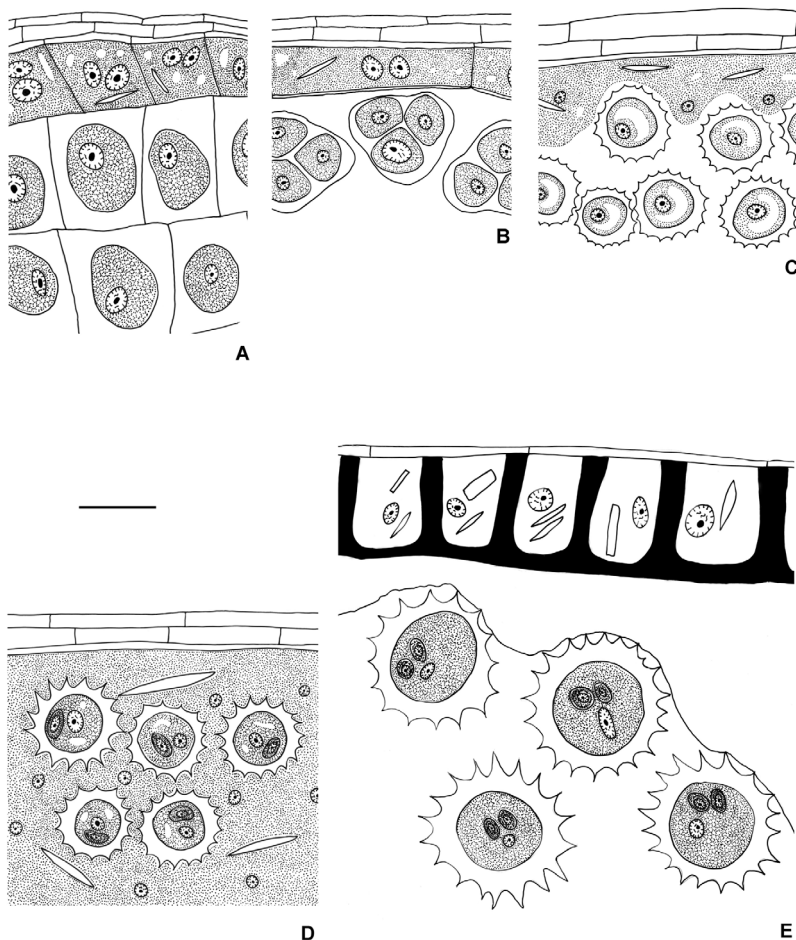


**Fig. 3.** DK 4050. Microsporangium tissues in different stages of development. — **A:** Microspore mother cell stage, binucleate tapetum with styloid crystals. — **B:** Tetrahedral tetrads, middle layer mostly degraded. — **C:** Free microspore stage, tapetum invading the anther locule. — **D:** Bicellular pollen-grain stage, thick epidermal cuticle visible, tapetum completely integrated. — **E:** Three-celled pollen grains, endothecium cells with fibrous thickenings and prismatic and styloid crystals, peritapetal membrane present. Scale bar 18  $\mu$ m.

10C). As the ovule grows the nucellus degenerates and, in HA 89, CF 17 and P 30, is no longer present at the four nuclei gametophyte stage while it persists in DK 4050 until the mature gametophyte stage. Once the nucellus has degenerated the endothelium comes in direct contact with the female gametophyte and covers its entire length.

### Megasporogenesis and megagametogenesis

Parietal cells are absent and the megaspore mother cell (MMC) is present just below the nucellar epidermis (tenuinucellate ovule). Ovules present a single MMC with a conspicuous nucleus and a prominent nucleolus (Figs. 6A, 8A, 10A, 13A).

The MMC divides meiotically, giving rise to a linear megaspore tetrad (Fig. 8B, 13B). The three micropylar megaspores degenerate and the chalazal one develops into a megagametophyte (Figs. 6B, 10C, D, 13C).

The functional megaspore enlarges (Figs. 6C, 8C, 10D) and its nucleus undergoes a first mitotic division unaccompanied by wall formation. The resulting nuclei are pushed to opposite poles by a central vacuole (Figs. 6D, 10E). A further mitotic karyokinesis gives rise to a four-nucleate female gametophyte, with two nuclei in each pole (Fig. 13D). Four-nucleate gametophytes of DK 4050 vary in length and have a more vacuolated cytoplasm than the other genotypes (Figs. 6E, 10F, G). After a last mitotic division, cytokinesis takes place and a young six-celled gametophyte with an egg apparatus, a central cell and two antipodals, is formed (Fig. 11A–C). The young

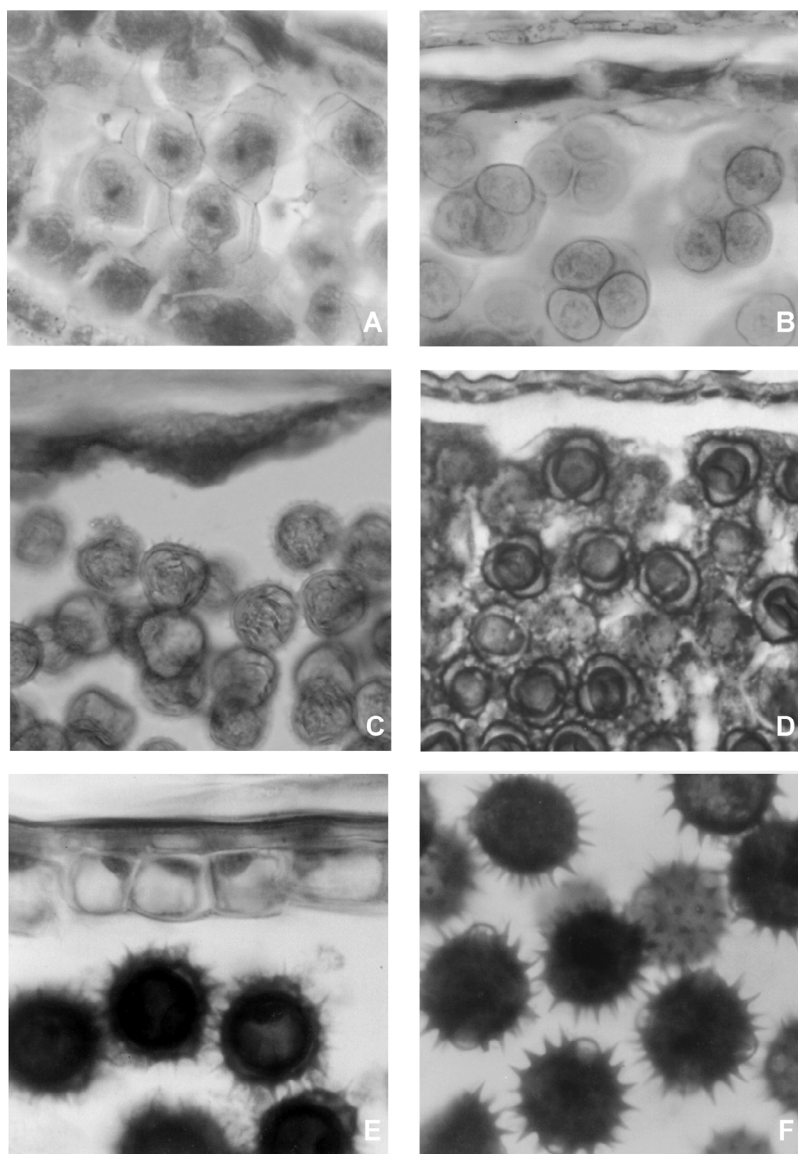


**Fig. 4.** *Helianthus annuus*. **A–E:** Microsporogenesis and microgametogenesis in CF 17 and P 30. **F:** HA 89. — **A:** Microspore mother cells. — **B:** Microspore tetrads with a tetrahedral arrangement. — **C:** Free microspore stage. — **D:** Young microspores, plasmodial tapetum. — **E:** Bicellular pollen grains. — **F:** Tricellular pollen grains of HA 89 with four pores. Scale bars: **A** = 36  $\mu\text{m}$ , **B** = 32  $\mu\text{m}$ , **C** = 28  $\mu\text{m}$ , **D** = 18  $\mu\text{m}$ , **E** = 39  $\mu\text{m}$ , **F** = 31  $\mu\text{m}$ .

gametophyte varies considerably in size in DK 4050 (121–194  $\mu\text{m}$ ) (Fig. 11A, B) while on the other genotypes only large ones (160–190  $\mu\text{m}$ ) were observed (Figs. 7A, 8D).

Synergids of the young female gametophyte are short, with a dense cytoplasm and prominent nuclei (Fig. 11A–C). Vacuoles, when present, are at the chalazal end (Fig. 7A). As soon as the gametophyte forms, the synergids start to elongate (Figs. 7B, 8D, 12A). In the mature gametophyte, where synergids reach their maximum

size, nuclei may position in the micropylar region of the synergids (Figs. 7C, D, 8D), in the middle of the cells (Figs. 8E, 9A–C, 11D, 12B–D) or in the chalazal end (Figs. 7E, 8F, 9B, D, 12E).

The young female gametophyte presents a more or less round egg cell with a dense cytoplasm and may have a vacuole (Figs. 7A, B, 8D, 12A) or not (Fig. 11A–C). The egg cell of the mature female gametophyte is larger, oblong and has a large vacuole which pushes the conspicuous nucleus towards the chalazal region (Figs.

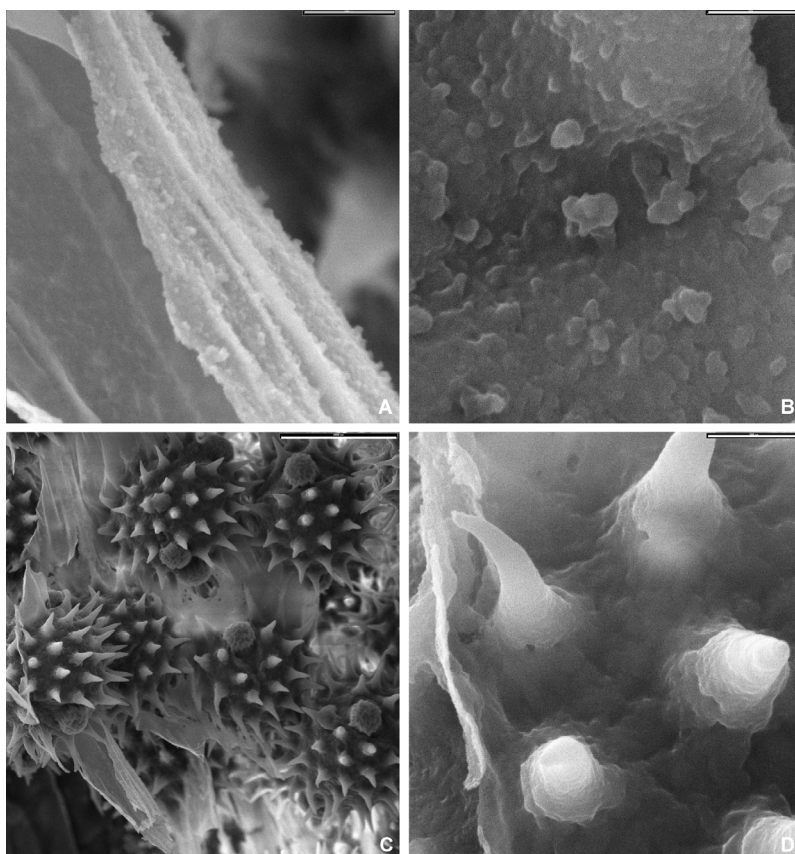


**Fig. 5.** *Helianthus annuus*. Ubisch bodies and pollen grains. MEB in P 30. — **A**: Peritapetal membrane with Ubisch bodies or orbicules. — **B**: Detail of the orbicules. — **C**: Pollen grains and peritapetal membrane. — **D**: Detail of the exine. Scale bars: **A**, **C** = 2000 nm, **B** = 1000 nm, **D** = 20 000 nm.

7C–E, 8E, F, 9A–D, 11B, 12B–E). The egg apparatus in DK 4050 grows towards the micropyle and out of the endothelium.

The young central cell contains two polar nuclei, which may be separated by a large central vacuole as in CF 17 and P 30 (Fig. 8D) or close to each other as in DK 4050 (Fig. 11A and B). They fuse before the gametophyte starts to elongate (Fig. 7A). The secondary nucleus is, in most cases, quite large with a very conspicuous nucleolus (Figs. 7B, C, 8F, 9C, D, 11D, 12A, B, D, E). The large vacuole of the young central cell remains as such in CF 17 and P 30 (Figs. 8E, F, 9A–D, 13F), while in most megagametophytes of DK 4050 many small vacuoles may form (Figs. 11C, 12B, D, E). The cytoplasm of the central cell in HA 89 is the least vacuolated (Fig. 7C, E). In all genotypes the mature central cell prolongs towards the micropylar end enclosing the egg cell and the synergids (Figs. 7C, 8F, 9C, D, 12B–E, 13F).

All young gametophytes have only two antipodals (Figs. 7A, 8D, 11A, B). In young megagametophytes of DK 4050 the micropylar antipodal contains two nuclei, while the chalazal antipodal has only one (Fig. 11A–C). At the following stage of its development four and two nuclei are present in each antipodal respectively (Fig. 12A). The number of nuclei in these cells increases with the maturation of the gametophyte (Figs. 11D, 12B–E). Although mature megagametophytes with two antipodals are more frequent in DK 4050 (Figs. 11D, 12B–D) gametophytes with four antipodals also exist (Fig. 12E). The other genotypes have gametophytes where the amount of nuclei is independent of the developmental stages (Figs. 7B–E, 8E, F, 9A–D). P 30 remains always with only two antipodals (Fig. 9A–D), CF 17 may present two or four (Fig. 8D–F), while in HA 89 there are megagametophytes with two, three and four antipodals (Fig. 7B–E). There are thick walls



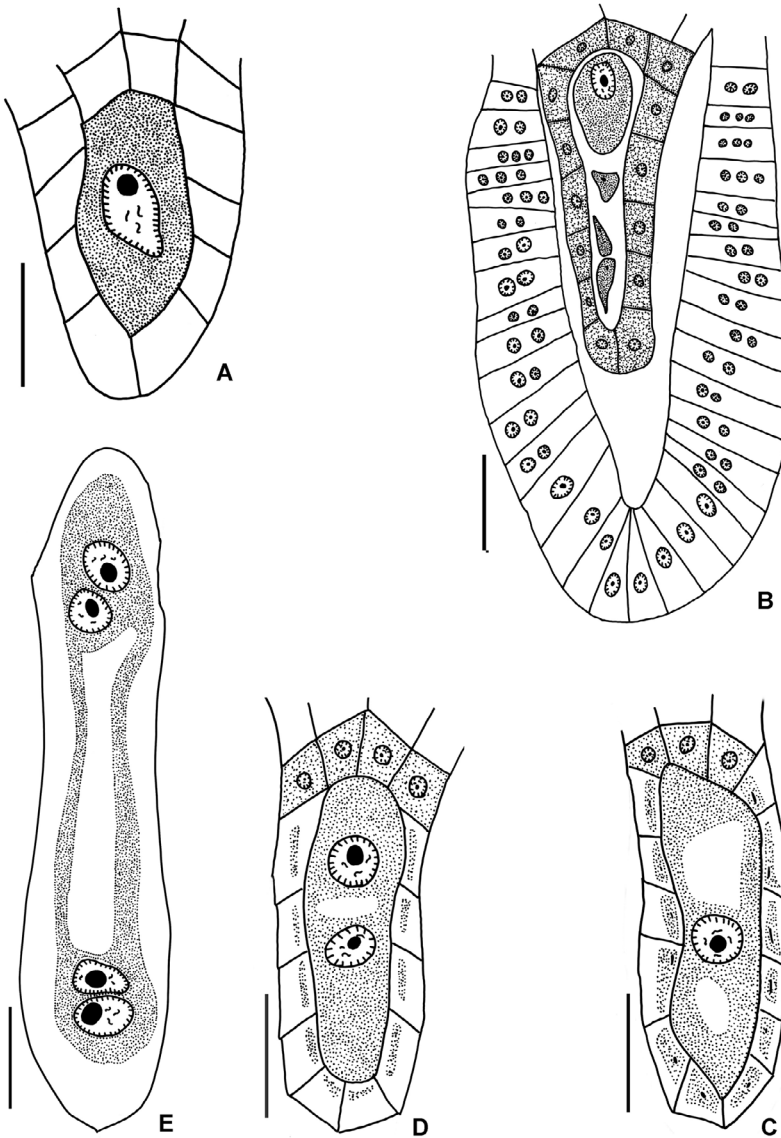


**Fig. 6.** *Helianthus annuus* (HA 89). — **A:** Megaspore mother cell, tenuinucellate ovule. — **B:** Linear megaspore tetrad, chalazal megaspore functional and micropylar ones degenerating, nucellar epidermis, endothelium developed with up to three nuclei in each cell. — **C:** Functional megaspore, nucellus partly consumed. — **D:** Two-nucleate gametophyte, nucellus cells mostly disintegrated. — **E:** Four-nucleate gametophyte. Scale bars 18 µm.

separating the antipodals from the central cell and from each other in all female gametophytes of P 30 (Figs. 9A–D, 13E) and in most of HA 89 and CF 17 (Figs. 7A–C, E, 8E, F). On the other hand, DK 4050 presents such walls occasionally, only in mature gametophytes, either separating the last antipodal (Fig. 12D) or the central cell from the micropylar antipodal (Fig. 12E).

## Fertilization

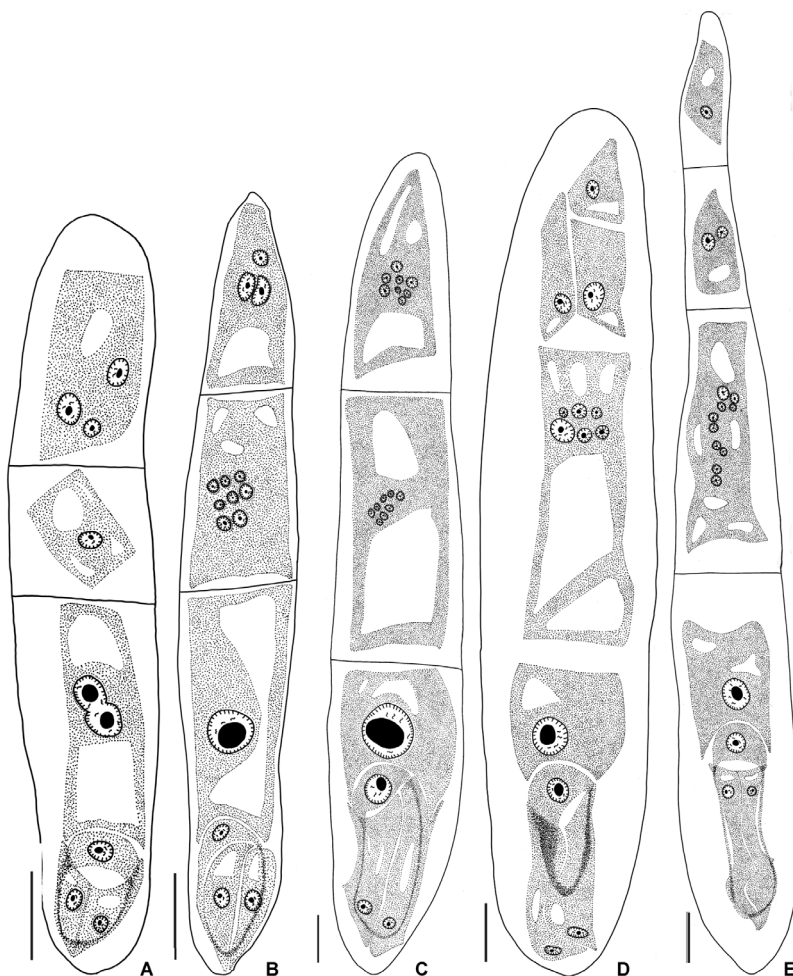
The pollen tube grows into one of the syn-

ergids, where both sperms are released. One male gamete fuses with the nucleus of the egg cell to form the zygote. The fusion of the second male gamete with the polar nuclei results in the endospermogenetic cell.

At this stage, the endothelium, which originally had a single layer of cells, starts to develop further layers in all the hybrids while in HA 89 it remains the same. Hybrids may present an endothelium with up to six cell layers surrounding the antipodals. It starts to isolate antipodals from each other and the central cell.



**Fig. 7.** *Helianthus annuus* (HA 89). — **A:** Young megagametophyte, polar nuclei fusing, two antipodals. — **B:** megagametophyte, polar nuclei fused. — **C:** Mature megagametophyte, synergids nuclei in the micropylar region. — **D:** Mature megagametophyte, thick walls separating the antipodals from the central cell and from each other absent, four antipodals. — **E:** Mature megagametophyte with three antipodals. Scale bars 18  $\mu\text{m}$ .



## Discussion

Anther wall development is of the dicotyledonous type described by Davis (1966), which was observed in the Asteraceae (Pullaiah 1979). The tapetum was similarly described by Horner (1977) and is common to other members of the family (Pullaiah 1979). *Helianthus annuus* has a *Selaginella*-type plasmodial tapetum since it is completely integrated at the bicellular pollen-grain stage.

The peritapetal membrane that encloses pollen grains and the Ubisch bodies or orbicules on its inner surface were not mentioned on previous accounts of the microsporogenesis and microgametogenesis of *H. annuus* (Horner 1977, Szabó *et al.* 1984, Laveau *et al.* 1989).

Yet, Szabó *et al.* (1984) reported an intermediate status between the endothecium and the locule of an open anther. Heslop-Harrison (1969) observed such membrane on *Cosmos bipinatus* (Heliantheae), *Ambrosia artemisifolia* (Ambrosieae) and *Tagetes patula* (Helenieae). Nevertheless, he made no reference to the presence of orbicules. Even though the orbicule functions are still poorly understood they are considered by most authors to be exclusive of secretory tapeta (Raghavan 1997, Huysmans & El-Ghazaly 1998, Furness & Rudall 2001). Strittmatter *et al.* (2000) described, on an ultrastructural ontogenetic study on pollen development of *Abutilon pictum* a peritapetal membrane with orbicules in the mature anther. In that species, orbicules as well as the membrane are formed from a

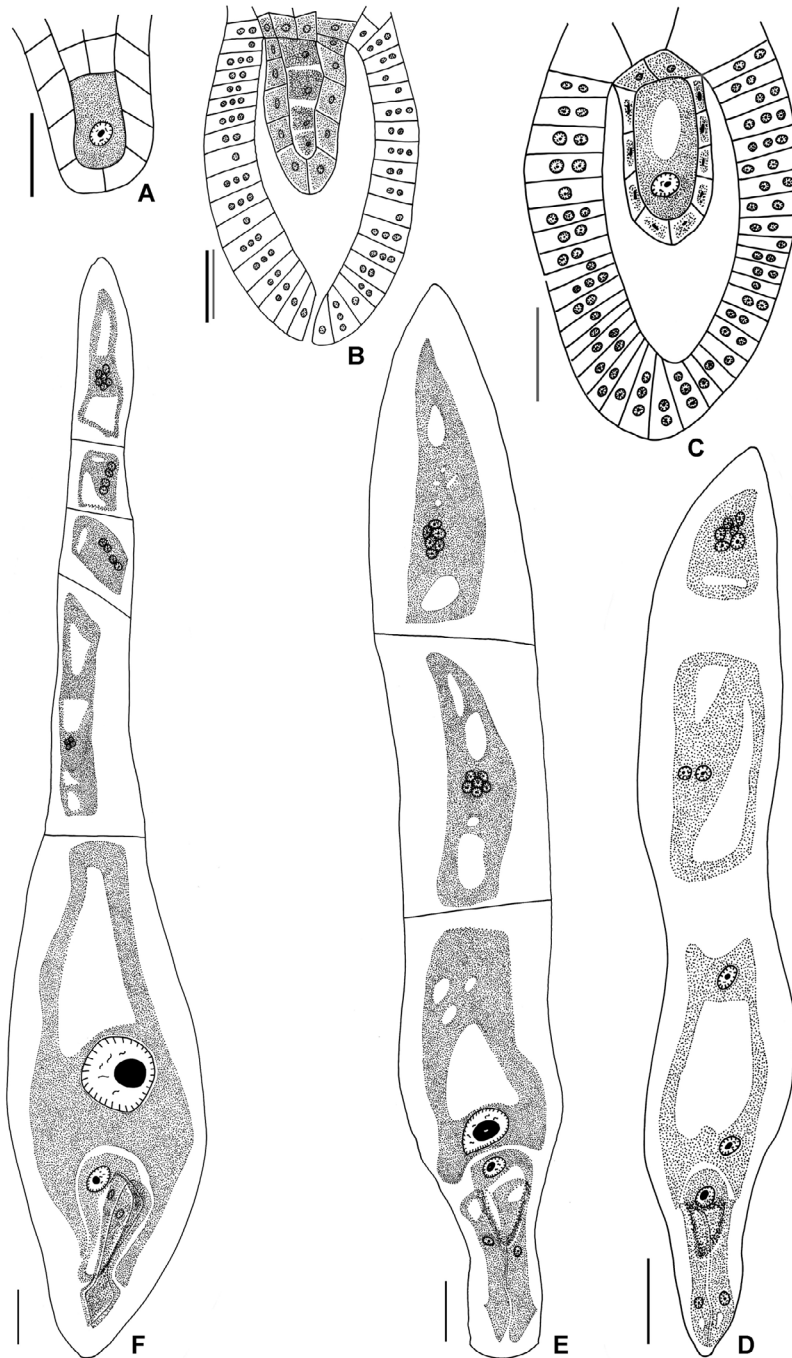


**Fig. 8.** *Helianthus annuus* (CF 17 and P 30). — **A:** Megaspore mother cell, tenuinucellate ovule. — **B:** Linear megaspore tetrad, nucellar epidermis, endothelium developed with up to three nuclei in each cell. — **C:** Functional megaspore, nucellus partly consumed. — **D:** Young megagametophyte, polar nuclei not fused, thick walls separating the antipodals from the central cell and from each other absent. — **E:** Mature megagametophyte with two antipodals. — **F:** Mature gametophyte with four antipodals. Scale bars 18  $\mu\text{m}$ .

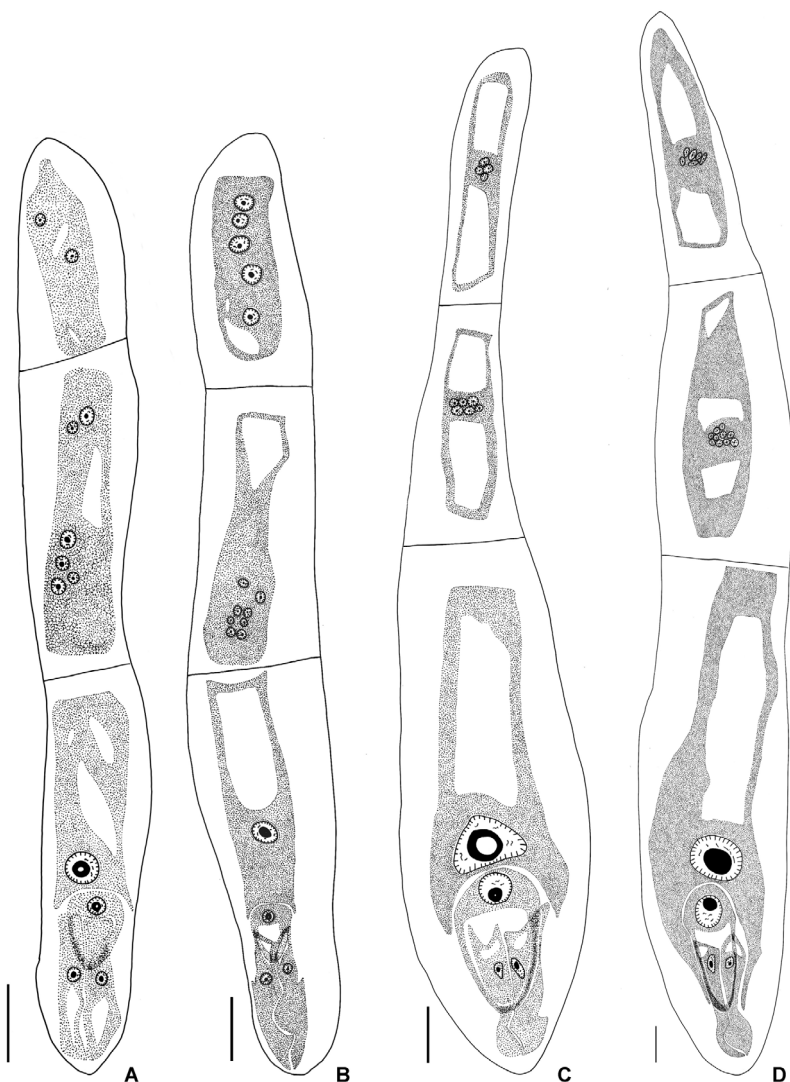
plasmodial type tapetum, as in *H. annuus*. These are the first species of angiosperms where the presence of orbicules associated to a peritapetal membrane is reported.

Meric and Dane (2004) found calcium oxalate styloid crystals in the tapetum and endothelial

cells in *H. annuus*. However, young endothelial cells of HA89 and mature cells of DK4050 have prismatic crystals as well.

In *H. annuus* pollen mother cells divide simultaneously and produce tetrahedral pollen tetrads, as in *Vernonia divergens* and *Adenostema*

**Fig. 9.** *Helianthus annuus* (CF 17 and P 30). — **A:** Mature megagametophyte, synergids with chalazal nuclei and micropylar vacuoles. — **B:** Mature megagametophyte, synergids nuclei in the chalazal end. — **C:** Mature megagametophyte, conspicuous polar nucleus with a nucleolar vacuole. — **D:** Mature megagametophyte, central cell with a large vacuole, two antipodals with numerous nuclei. Scale bars 18  $\mu$ m.



*lavenia*, while in *Elephantopus scaber* (Vernoniaeae) and *Adenostema rugosum* (Eupatorieae), pollen tetrads have an isobilateral arrangement (Pullaiah 1979).

Szabó *et al.* (1984) observed between two and four pores in pollen grains of CR-3 restorer paternal line flowers of *Helianthus*. We found either triporate or tetraporate pollen grains in the line, while the hybrids only present triporate grains. Although microspores differ in size among the genotypes studied during different stages of their development, the hybrids present three-celled pollen grains larger than the ones in the line.

According to Laveau *et al.* (1989) the pollen grains of two fertile lines, HA89 and RHA 274 PL, were two-celled when released, the second mitosis occurring in the pollen tube. Yet, in all the genotypes of *H. annuus* that we studied, pollen grains are shed at the tricellular stage, as observed in most members of the family (Pullaiah 1979, Johri *et al.* 1992).

*Helianthus annuus* has an inferior, bicarpelar and unilocular ovary, with a single ovule, which is anatropous, unitegmic and tenuinucellate as in other members of the family (Pullaiah 1979). Pullaiah (1979) mentioned the occurrence of two ovules per ovary in about 3% of the ovaries of



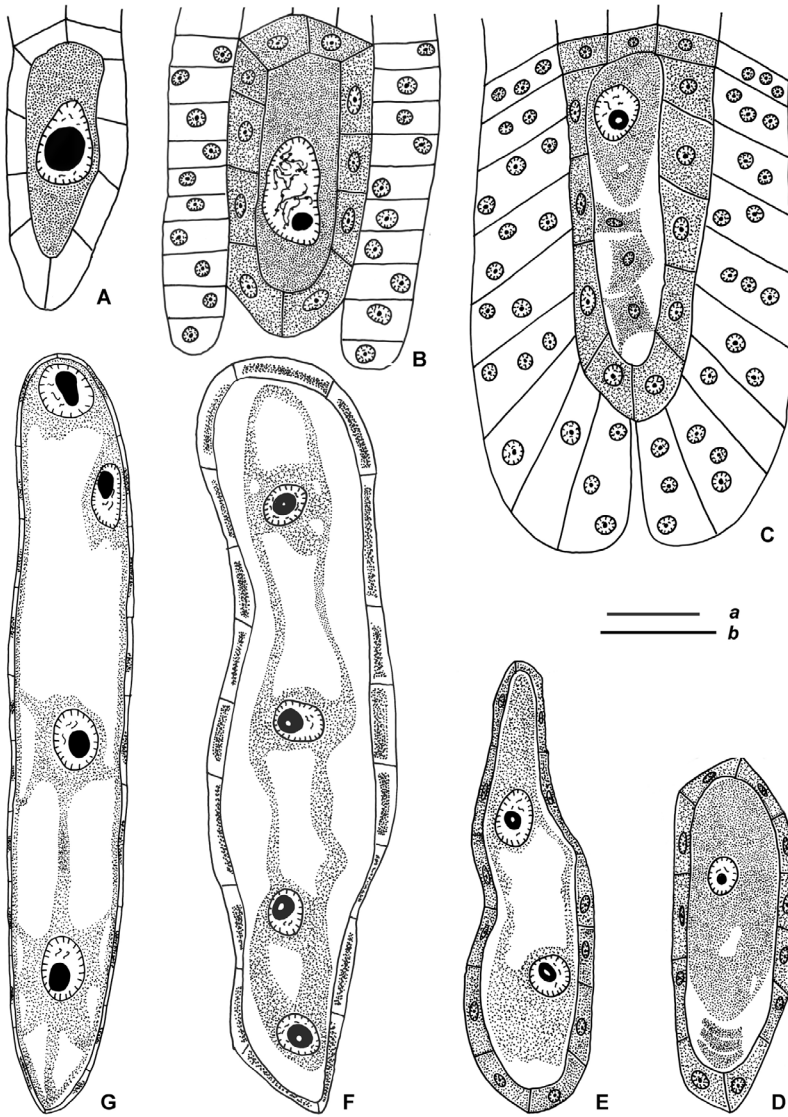


**Fig. 10.** *Helianthus annuus* (DK 4050). — **A:** Megaspore mother cell, tenuinucellate ovule; scale bar b. — **B:** Megaspore mother cell, nucellar epidermis, endothelium developed with a single nucleus in each cell; scale bar b. — **C:** Linear tetrad, endothelial cells with up to three nuclei per cell; scale bar b. — **D:** Functional megaspore and micropylar ones degenerating; scale bar b. — **E:** Two-celled megagametophyte, nucleus still present; scale bar b. — **F:** Short four-celled megagametophyte, nucellar cells partly consumed; scale bar b. — **G:** Large four-celled megagametophyte, nucellar cells partly consumed; scale bar a. Scale bars 18  $\mu$ m.

*Elephantopus scaber*. This feature appears in the genotypes studied along with two or three locules and two or three styles.

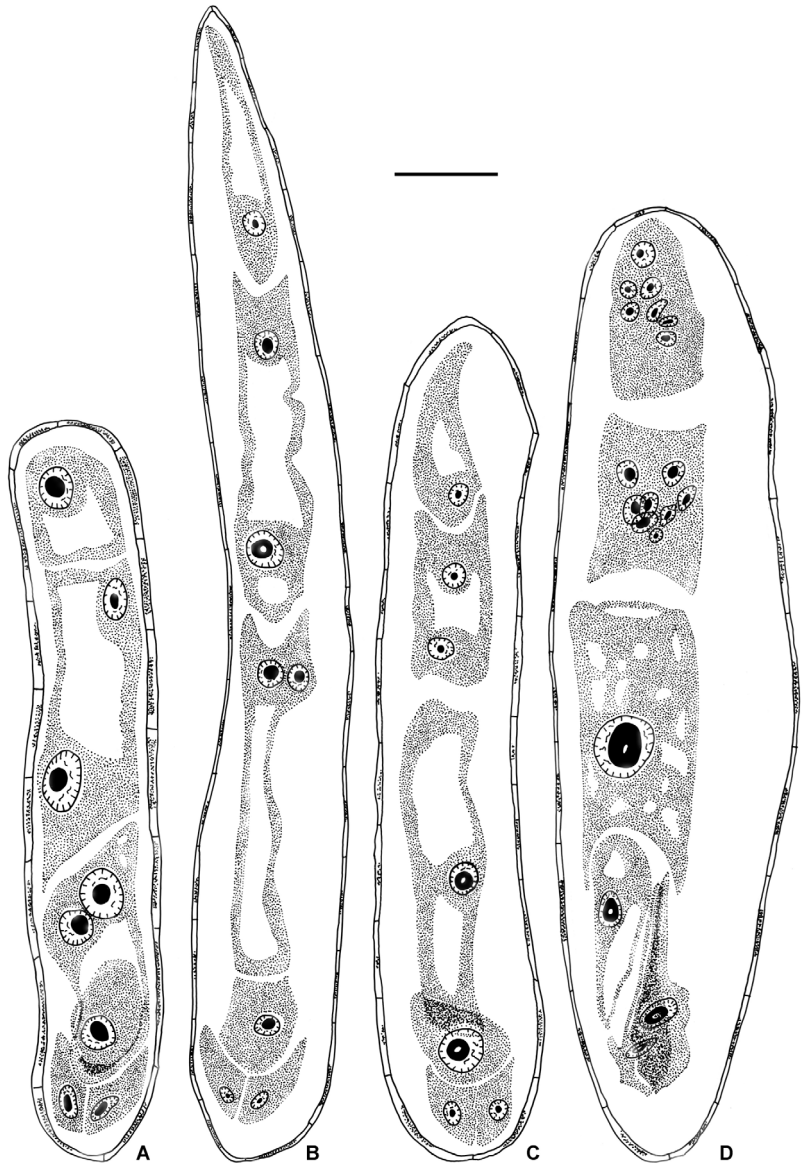
Newcomb (1972a) reported that at the megaspore mother cell stage the endothelium is differentiated as a single layer of darker staining cells surrounding the sides and micropylar portion of the nucellar tissue as in the hybrid DK 4050. However, the inner epidermis of the integument of the other genotypes elongates radially, becomes glandular and functions as the integumentary tapetum at the megaspore tetrad stage, in concordance with the observations of Pullaiah

(1979) for members of the tribes Vernoniaeae and Eupatorieae. Newcomb (1972a) reported only few bi-nucellate endothelium cells due to the misformation of the cell wall separating the two nuclei, whereas cells of the genotypes here studied had between two and three nuclei.

Nucellar cells start to degenerate at the binucellate gametophyte stage and almost disappear at the tetranucellate gametophyte in CF 17, P 30 and HA 89 in concordance with Newcomb's (1972a) observations. However, nucellar cells of DK 4050 do not fully degenerate until the complete formation of the gametophyte and fusion of



**Fig. 11.** *Helianthus annuus* (DK 4050). — **A:** Short young megagametophyte, both polar nuclei in the central cell, micropylar antipodal with two nuclei and chalazal antipodal with a single nucleus. — **B:** Large young megagametophyte, polar nuclei of the central cell not fused yet, micropylar antipodal with two nuclei and chalazal antipodal with a single nucleus. — **C:** Megagametophyte, polar nuclei fused, micropylar antipodal with two nuclei and chalazal antipodal with a single nucleus. — **D:** Megagametophyte, antipodals with numerous nuclei, rest of nucellar cells still present. Scale bar 18  $\mu$ m.



the polar nuclei.

Throughout the development of the female gametophyte all nuclei contain a single nucleolus that may develop a large vacuole. Previously this was mentioned only for the egg and central cell (Newcomb 1972a, Yan *et al.* 1990).

The four-nucleate gametophyte of HA89 presents a large central vacuole that leaves a thin layer of cytoplasm that connects the chalazal region to the micropylar region. Each end of the cytoplasm has two nuclei. Newcomb (1972a) provided a similar description. On the other

hand, gametophytes of DK 4050 at same stage contain a less dense cytoplasm with numerous and large vacuoles separating the four nuclei from each other. This hybrid shows variation in the sizes of the four-nucleate gametophytes.

We did not find an eight-nucleate gametophyte despite the high number of flowers (approximately 30 for each genotype) in such stage of development analyzed. Neither did Newcomb (1972a), who suggested that this might be because divisions occur rapidly or at night. We collected and fixed flowers at different times of

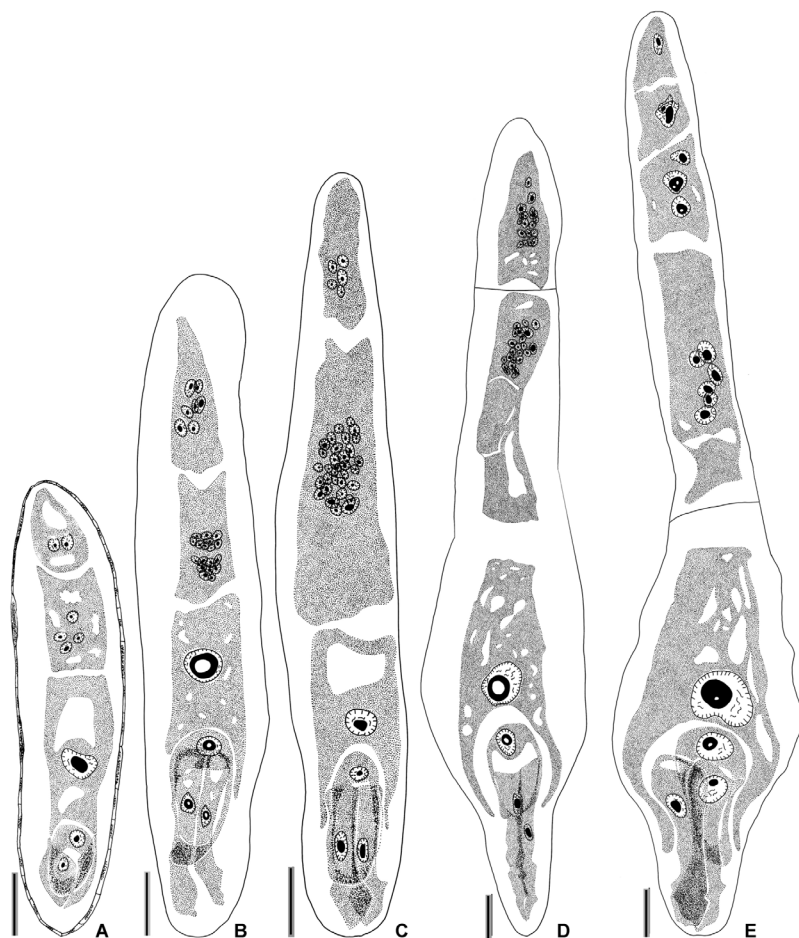


**Fig. 12.** *Helianthus annuus* (DK 4050). — **A:** Megagametophyte, conspicuous polar nucleus, four nuclei in the micropylar antipodal and two in the chalazal one. — **B:** Mature megagametophyte, nucellus completely absent, polar nucleus with a nucleolus vacuole. — **C:** Mature megagametophyte, synergids nuclei in the middle of the cells, both antipodals with numerous nuclei. — **D:** Mature megagametophyte, polar nucleus with a nucleolus vacuole, thick wall between the antipodals. — **E:** Mature megagametophyte, thick wall between the central cell and the micropylar antipodal, four antipodals. Scale bars 18  $\mu$ m.

the day in order to find the missing stage. We conclude that cytokinesis takes place during the third mitosis, resulting in a six-celled gametophyte of the same size as the four-nucleate one.

Newcomb (1972a) and Yan *et al.* (1991) based most sunflower synergid descriptions on mature gametophytes. In the young gametophytes they are short, with a dense cytoplasm and prominent nuclei. Synergids of mature megagametophytes have different polarities. However, the vacuoles are mostly in the chalazal end and nuclei in the centre of the cells, coinciding with previous accounts (Newcomb 1972a, Yan *et al.* 1990).

Two antipodals are present in the young gametophyte of *H. annuus* in contrast to the usual occurrence of three antipodals in the normal *Polygonum*-type (Maheshwari 1950). Newcomb (1972a) mentioned this in his report.

*Adenostemma rugosum*, *A. lavenia*, *Verno-*

*nia elaeagnifolia* and *V. divergens* have either two or three antipodals. When two, the upper one is always binucleate (Pullaiah 1979), as we observed in the female gametophytes of DK 4050. Even though most mature gametophytes remain with two antipodals, several develop three or four, probably by a later division of the original ones. In all cases, the number of nuclei increases in the micropylar antipodal cell and sometimes in all. Ustinova (as cited in Newcomb 1972a) and Newcomb (1972a) described similar variations, although the former claimed that the antipodals develop from three cells located in the chalazal region, of which the micropylar cell usually degenerates. We did not observe similar features. Newcomb (1972a) mentioned the presence of occasional freely growing walls extending partially across the central cell. P30, CF 17 and HA 89 had in most gametophytes very thick

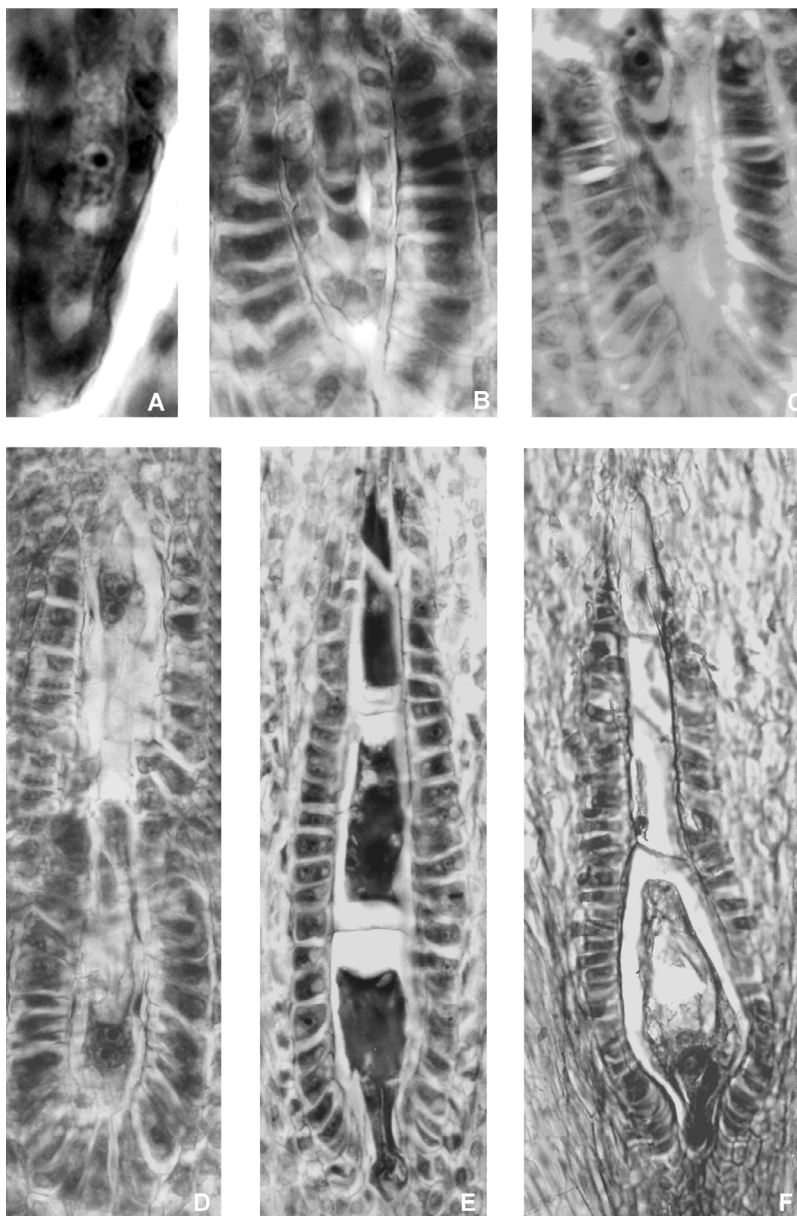


**Fig. 13.** *Helianthus annuus*. Megasporogenesis and megagametogenesis in CF 17 and P 30. — **A:** Megaspore mother cell. — **B:** Linear megaspore tetrad. — **C:** Functional megaspore and degenerative micro-pylar ones. — **D:** Four nuclei megagametophyte. — **E:** Megagametophyte with three antipodals and thick walls between them and them and the central cell. — **F:** Mature megagametophyte, central cell with a large vacuole, endothelium surrounding most of the gametophyte. Scale bars: **A** = 13  $\mu\text{m}$ , **B** = 28  $\mu\text{m}$ , **C** = 29  $\mu\text{m}$ , **D** = 42  $\mu\text{m}$ , **E** = 54  $\mu\text{m}$ , **F** = 50  $\mu\text{m}$ .

antipodal cell walls, whereas such walls are rare in DK 4050.

Newcomb (1972b) observed an increase in the size of endothelium cells after fertilization, as we did for the hybrids studied, along with an increase in the amount of cell layers. However, this was not the case for HA 89. The growth of that tissue may be due to the passage of nutritive substances from the antipodals that will later supply the young embryo and endosperm. In all,

the differences between the genotypes we studied may justify the contradictions found in previous accounts. It is also concluded that all the female gametophytes here described may be fertilized and may produce viable seeds. Therefore, we cannot adjudicate the abortion of fruits to abnormalities in the development of the gametophyte. We will continue our research analyzing post-fertilization events and seed formation in order to look for the possible causes of fruit abortion.

## Acknowledgements

We thank Dr. María Teresa Amela Gacía and Dr. Patricia Hoc for a critical reading of the manuscript and assistance with the English language.

## References

- D'Ambrogio, A. 1986: *Manual de técnicas en histología vegetal*. — Hemisferio Sur S.A. Buenos Aires.
- Davis, G. L. 1966: *Systematic embryology of the angiosperms*. — John Wiley & Sons, New York.
- Furness, C. A. & Rudall, P. J. 2001: The tapetum in basal angiosperms: early diversity. — *Int. J. Plant Sci.* 162: 375–392.
- Heslop-Harrison, J. 1969: An acetolysis-resistant membrane investing tapetum and sporogenous tissue in the anthers of certain Compositae. — *Can. J. Bot.* 47: 541–542.
- Horner, H. T. 1977: A comparative light- and electron-microscopic study of microsporogenesis in male-fertile and cytoplasmic male-sterile sunflower (*Helianthus annuus*). — *Am. J. Bot.* 64: 745–759.
- Huysmans, S. & El-Ghazaly, G. 1998: Orbicules in angiosperms: morphology, function, distribution, and relation with tapetum type. — *Bot. Rev.* 64: 240–272.
- Johri, B. M., Ambegaokar, K. B. & Srivastava, P. S. 1992: *Comparative embryology of angiosperms*, vols. 1 and 2. — Springer-Verlag, Berlin.
- Laveau, J. H., Schneide, C. & Berville, A. 1989: Microsporogenesis abortion in cytoplasmic male sterile plants from *H. petiolaris* or *H. petiolaris fallax* crossed by sunflower (*Helianthus annuus*). — *Ann. Bot.* 64: 137–148.
- Maheshwari, J. K. 1950: *An introduction to the embryology of angiosperms*. — McGraw-Hill, New York.
- Meric, C. & Dane, F. 2004: Calcium oxalate crystals in floral organs of *Helianthus annuus* L. and *H. tuberosus* L. (Asteraceae). — *Acta Biol. Szegediensis* 48(1–4): 19–23.
- Newcomb, W. 1972a: The development of the embryo sac of sunflower *Helianthus annuus* before fertilization. — *Can. J. Bot.* 51: 863–878.
- Newcomb, W. 1972b: The development of the embryo sac of sunflower *Helianthus annuus* after fertilization. — *Can. J. Bot.* 51: 879–898.
- O'Brien, T. P. & McCully, M. E. 1981: *The study of plant structure. Principles and selected methods*. — Termarcaphi Pty. Ltd., Melbourne.
- Pullaiah, T. 1979: Embryology of *Adenostemma*, *Elephantopus* and *Vernonia* (Compositae). — *Bot. Notiser* 132: 51–56.
- Raghavan, V. 1997: *Molecular embryology of flowering plants*. — Cambridge Univ. Press, Cambridge.
- Strittmatter, L. I., Galati, B. G. & Monacci, F. 2000: Ubisch bodies in peritapetal membrane of *Abutilon pictum* Gill. (Malvaceae). — *Beitr. Biol. Pflanzen* 71: 1–10.
- Szabó, M., Gulyás, S. & Frank, J. 1984: Comparative anatomy of the androecium of male sterile and fertile sunflowers (*Helianthus*). — *Acta Bot. Hungarica* 30: 67–73.
- Yan, H., Yang, H. Y. & Jensen, W. 1990: Ultrastructure of the developing embryo sac of sunflower (*Helianthus annuus*) before and after fertilization. — *Can. J. Bot.* 69: 191–202.